Asia-Pacific Journal of Chemical Engineering

WILEY | Curtin University

RESEARCH ARTICLE OPEN ACCESS

Optimization and Characterization of Aspirin- and Ibuprofen-Loaded Lipid-Based Nanoparticle Synthesis for Antibacterial Activity and Cytotoxic Effect

Gulizar Caliskan[1] | Smyrna Ergonul[1] | Zuhal Naz Cansu[2] | Busra Kaplan[2]

[1]Department of Genetics and Bioengineering, Faculty of Engineering, Izmir University of Economics, Izmir, Türkiye | [2]Department of Biomedical Engineering, Faculty of Engineering, Izmir University of Economics, Izmir, Türkiye

Correspondence: Gulizar Caliskan (gulizar.caliskan@ieu.edu.tr)

Received: 28 August 2025 | **Revised:** 22 October 2025 | **Accepted:** 24 October 2025

Keywords: central composite design | cytotoxic effects | drug-delivery | encapsulation efficiency | lipid extraction | lipid-based nanoparticles

ABSTRACT

Lipid-based nanoparticles (LNPs) are favored for drug delivery because of their low toxicity, high biocompatibility, ability to self-assemble into nanoparticles, and ability to enhance drug bioavailability, thereby improving drug release modulation and pharmacokinetics. In this study, the regional palm fruit extract and thyme oil were used as an oil source for the synthesis of LNPs with/without drugs. The Design Expert statistical software program, Central Composite Design (CCD) method was used to optimize the effect of drug:lipid ratio (1:3–1:7), drug type (ibuprofen or aspirin) and incubation time (5–15 min) on encapsulation efficiency (EE%), and antibacterial activity. The maximum EE% of 94% was achieved using ibuprofen at a drug:lipid ratio of 1:7 with a 5-min incubation time. Physicochemical characterization showed the inclusion of both aspirin and ibuprofen imparted a strong negative charge (up to −15 mV) and yielded average sizes ranging from 180 to 560 nm. Furthermore, ibuprofen- and aspirin-loaded LNPs exhibited promising cytotoxic effects on the hepatocarcinoma cell line (Huh7), showing 50% and 70% viability at a concentration of 50 μM, respectively. Ultimately, the demonstrated efficacy of palmitic acid–incorporated LNP formulations suggests a significant potential for these optimized carriers to improve the therapeutic efficacy of antitumor drugs in clinical applications.

1 | Introduction

Lipid-based nanoparticles (LNPs), characterized by their hydrophilic and hydrophobic regions, have great potential for cancer treatment for several reasons: They increase the half-life of anticancer drugs in the bloodstream because of their ease of surface modification, hydrophilic and hydrophobic drug loading potential, high biocompatibility, high interaction with a high surface/volume ratio, and amphiphilic structure [1–4]. In addition, these nanoparticles can support physical stability, have high drug loading capacity, are easy to scale up, and do not require the use of organic solvents. Thus, they are currently used in biotechnological fields, such as medical and photoacoustic imaging technologies [5], nanotechnology, pharmaceutical industry, cosmetics industry, nutrition, and agriculture, as well as having innovative uses in fields such as cosmetics industry, nutrition, and agriculture.

LNPs consisting of one or more lipid layers are used in the delivery and release of lipid-soluble and amphiphilic substances to the target site by allowing encapsulation of lipid-soluble and amphiphilic substances because of both aqueous phase and lipids in their structure [1, 3, 6]. One type of LNPs includes liposomes, solid lipid nanoparticles (SLNs), and nanostructured lipid carriers (NLCs), cationic lipid–nucleic acid complexes. These are used to deliver various therapeutics,

such as anticancer drugs and vaccines, by improving drug loading, diffusion across biological barriers, and targeting properties [7].

Such properties have made LNPs a promising target for targeted therapy. They protect the loaded cancer drugs from oxidation and degradation by forming a phospholipid barrier against biological secretions and enzymes, while ensuring adequate therapeutic drug concentrations in the tumor's microenvironment [2, 8, 9]. Overall, LNPs present a promising avenue for advancing pharmaceuticals through efficient and targeted drug delivery systems with enhanced therapeutic effectiveness and reduced side effects [10–12].

There are various lipid sources and processes used in the synthesis of LNPs employed in drug delivery systems. Generally, LNPs are produced using organic solvent-free methods such as ultrasonication, high-pressure homogenization, high-speed mixing, phase inversion, emulsion/solvent evaporation, solvent injection, and double emulsion [9, 13–15]. Examples of preferred lipid components in LNP formation are fatty acids, fatty alcohols, glycerides, stearic acid, and liquid fats and waxes such as glycerol triacrylate, ethyl oleate, isopropyl myristate, glycerol dioleate, and oleic acid. Lipid–water interface surfactants reduce the interfacial tension between the aqueous phases and lipid and also increase the stability of the resulting formulations. Surfactants/emulsifiers commonly used in LNP preparation are lecithin, poloxamer 188-407, tyloxapol, polysorbate 20-60-80, sodium (glyco)cholate, Tween80, and so forth [9, 11, 16].

Palm oil, which includes essential compounds, fatty acids, and phytonutrients such as carotenes, tocopherol, and tocotrienol, is a natural oil containing many important compounds and fatty acids easily exploitable in lipid-based formulations and drug delivery. A lipid-based formulation using palm oil has the potential to eliminate problems associated with current drug systems, such as hydrophobicity, lipophilicity, low bioavailability, drug permeability, and solubility [17]. However, there is little research on the application of palm oil and its fractions in lipid-based formulation. The present study therefore seeks to explore the research and findings on incorporating regional palm oil into lipid-based formulations and drug delivery systems, emphasizing the significance of assessing its potential and advantages. Current research areas related to the use of palm oil–based nanoparticles include their application in fields such as nanocomposite processing, environmental remediation, construction composite materials, catalysis, and various bioengineering applications, including cancer therapy, biomedical research, drug delivery, and nutraceutical formulations [18–20]. One future research direction is a focus on enhancing drug delivery through various mechanisms. Studies have demonstrated that SLNs and NLCs containing palmitic acid can be designed with specific properties, such as a size of 250 nm, negative zeta potential, and controlled release capabilities. These attributes contribute to improved drug bioavailability and intracellular delivery [18, 20]. These nanoparticles can be engineered so that they are able to interact effectively with physiological fluids, remain stable, and exhibit enhanced cellular uptake capacity, ultimately leading to improved drug delivery into the oral mucosa [18]. Additionally, the use of palmitic acid in nanoparticle formulations has been shown to enhance drug stability, sustained release, and mucosal delivery, overcoming biological barriers such as gastrointestinal degradation and mucus barriers, making them promising for the oral administration of hydrophobic drugs, thereby improving therapeutic efficacy, reducing cancer cell viability, and promoting tissue repair [20–22].

Optimization of parameters such as lipid and surfactant concentrations, drug, environmental conditions (temperature, etc.), incubation time, and mixing rate is crucial for obtaining nanoparticles with desired characteristics, such as small size and narrow distribution, and is of critical importance in the synthesis of LNP [9]. In this study, various techniques were used to optimize the synthesis of LNPs using thyme oil and palm oil extracted from the regional palm fruits (see Supporting Information). The Design Expert program was used for optimization in the synthesis of LNPs. The effect of drug:lipid ratio (1:3–1:7), drug type (ibuprofen or aspirin), and incubation time (5–15 min) on encapsulation efficiency (EE%), antibacterial effects on *Escherichia coli* and *Staphylococcus aureus* bacteria were investigated and optimized by Surface Response Method, Central Composite Design. This program was used to establish 22 experimental sets, after which optimization studies were initiated. The aim of the study is the characterization of LNPs synthesized with different drug contents, determining the potential for use in biotechnology and reaching the optimum production process, contributing to the literature with the first study on palm oil used in this way. Incorporating palmitic acid into LNP formulations has shown promising results in enhancing encapsulation efficiency, antibacterial activity, and cytotoxic effect on the hepatocarcinoma cell line (Huh7).

2 | Materials and Methods

2.1 | Lipid Extraction

The palm oil acquired from the fruits of local palm trees (*Elaeis guineenis*) in İzmir and the thyme oil used for the synthesis of lipid nanoparticles were selected for their suitability for the intended use, easy availability, saturation levels, and lipid structures. Approximately 100 g of palm fruit samples were washed, dried, and ground. Subsequently, ultrasound-assisted extraction of the ground palm lipid extracts was performed using 95% ethanol in 1 L [23]. The sample and solvent mixture was subjected to the extraction procedure in an ultrasonic bath with an integrated temperature control system (Jeiotech, US Portable Cleaners). The procedure was maintained for 10 min at a high sound level and a temperature of 20°C ± 2°C. The mixture was kept on a magnetic stirrer for 24 h, and the residue was vacuum filtered using a Whatman No. 1 filter.

The solution was then placed in a rotary evaporator at 9000 rpm, 60°C for 45 min to obtain palm oil. After solvent evaporation, the resulting material was considered and named as a lipid extract (palm oil). This content was also characterized to better understand the ingredients of palm oil with Gas Chromatography (GC) (Shimadzu GC 2030 Nexis, Japan). 0.1 g of palm oil was weighed, and 10 mL of hexane with 0.5 mL and 0.2 N KOH solution were added to the palm oil content [24]. After approximately 2 h, the extracted solution was analyzed on a Restek, Rxi-5ms (Crossbond 5%, diphenyl/95%, dimethylpolysiloxane), 30 m, 0.25 mmID, 0.25 μm df column with 0.2 mL/min nitrogen

gas, and the final determination was made in a flame ionization detector (FID).

2.2 | Synthesis of Drug-Loaded and Nondrug LNP

In this study, ultrasonication and high-speed mixing were combined for an effective and efficient synthesis process in the preparation of homogeneous LNPs [13, 25–28]. In general, LNP synthesis was performed by injecting the aqueous phase containing 1% w/v Tween 80 solutions into the lipid phase, magnetically stirred at 500 rpm, at a rate of 1 drop/s. The temperature of both phases was maintained at 75°C. For the synthesis of drug-loaded LNPs, either aspirin or ibuprofen was added to the aqueous solution in specific amounts according to the design. The effects of the drug:lipid ratio (1:3–1:7), type of drug (ibuprofen or aspirin), and incubation time (5–15 min) on encapsulation efficiency (EE%), as well as the antibacterial effects on *E. coli* and *S. aureus* bacteria, were optimized in Central Composite Design.

The obtained pre-emulsion was homogenized at high speed using the Ultra-Turrax T25 homogenizer at 8000 rpm for various incubation times (ranging from 5 to 15 min) at 75°C to prevent lipid crystallization. The final product was subjected to high-power sonication for 10 min at a constant temperature of 75°C. The mixture was first allowed to cool to room temperature and then subjected to centrifugation at 10000 rpm for 30 min at 4°C with the objective of separating the formed LNP from the medium. The LNPs, collected in pellet form and washed three times, were lyophilized for 48 h, and the drug-loaded and nondrug LNPs were stored at −20°C for characterization procedures.

2.3 | Encapsulation Efficiency (EE%)

To determine LNPs' incorporation capacity, according to the CCD, freeze-dried LNPs were dissolved in methanol, and the solution was analyzed directly for both aspirin and ibuprofen drugs using UV–vis spectrophotometry at 225 and 264 nm, respectively. Encapsulation efficiency (EE) was defined as follows [6, 21].

$$EE\,\% = (\text{Actual drug loading} / \text{Theoretical drug loading}) \times 100$$

2.4 | Statistical Analysis

The Design Expert program (version 13.0, Stat-Ease Inc., Minneapolis, MN) was used to optimize the production processes for the synthesis of LNPs. The Response Surface Methodology, Central Composite Design was employed to investigate and optimize the effects of the drug:lipid ratio (1:3–1:7), type of drug (ibuprofen or aspirin), and incubation time (5–15 min) on encapsulation efficiency (EE%), as well as the antibacterial effects on *E. coli* and *S. aureus* bacteria. Twenty-two trial runs with 20-mL working volume in Erlenmeyer flasks were conducted to initiate optimization studies. Differences between groups were analyzed using Student's *t*-test or one-way ANOVA, with Tukey's post hoc test applied for multiple comparisons. Statistical significance was defined as $p < 0.05$ (*), and a more stringent significance level was set at $p < 0.01$ (**).

2.5 | Characterization of LNPs

2.5.1 | UV–Visible Spectrophotometric Analyses

The surface plasmon resonances of drug-loaded and nondrug LNPs were scanned by UV–vis spectrophotometry (Perkin Elmer LAMBDA 750 UV/Vis/NIR) in the range of 250 and 800 nm [29]. The aspirin and ibuprofen stock solutions were prepared by taking 10 mg of each drug in 100 mL of pH 7.4 phosphate buffer. The drugs were dissolved in a solvent using a sonicator. Five different dilutions were prepared, with concentrations of 4,6, 8, 12, 16, and 50 μg/mL, respectively. Calibration curves were created for both aspirin and ibuprofen drugs at 225 and 264 nm, respectively.

2.5.2 | Fourier Transform Infrared Spectroscopy (FTIR) Analyses

In order to identify the functional groups associated with LNP formations, infrared spectra analysis was performed. This analysis was carried out using a PerkinElmer Spectrum FTIR Spectrometer in ATR mode at room temperature within the range of 400–4000 cm^{-1} [29].

2.5.3 | Dynamic Light Scattering (DLS) Analyses

Malvern Zeta Sizer NanoPlus Analyzer was used to determine zeta potential, hydrodynamic size distribution, the average harmonic mean particle diameter, and polydispersity index (PDI) value of drug-loaded and nondrug LNPs [30]. For each suspension, measurements were taken at room temperature and conducted in duplicates.

2.5.4 | Scanning Electron Microscopy (SEM) and Energy-Dispersive X-Ray Spectroscopy (EDX) Analyses

The morphology of LNPs coated with Au-Pd under 7.50 kV high vacuum was investigated using SEM (Thermo Scientific Apreo S.). The elemental composition of the LNPs was analyzed using EDX detectors.

2.6 | Antibacterial Activity Test

The disc diffusion method was used to assess the antibacterial activity of LNPs against Gram-negative *E. coli* and Gram-positive *S. aureus* [31]. In this study, gentamicin (Biochrom AG, 10 mg/mL) was utilized as the positive control, whereas nondrug LNPs served as the negative control.

2.7 | In Vitro Cytotoxicity and MTT Assay of LNPs

During a period of 48 h treatment, the in vitro cytotoxicity of LNPs was tested against the hepatocarcinoma cell line (Huh7), determined by 3-(4,5-dimethyl-2-thiazolyl)-2,5-diphenyl-2H-tetrazolium bromide (MTT) assay at different concentrations. The cells were seeded in 96-well plates containing 100 μL of DMEM

low glucose medium supplemented with 10% FCS, 1%P/S (50 units/mL penicillin and 50 μg/mL streptomycin) at 37°C in a humidified atmosphere of 5% CO_2 incubator. The cellular density was adjusted to be 5000 cells per well ($n = 3$).

Following cell seeding, the medium was substituted with a fresh medium containing the drug-loaded nanoparticles and Sorafenib. The samples were then incubated for 48 h. In detail, 15 μL of MTT solution (5 mg/mL, BioBasic-0793) was added to each well, and the cells were further incubated at 37°C for 4 h. The cell viability % was recorded under different treatment conditions, including a control group, two concentrations (100 and 50 μM) of ibuprofen- and aspirin-loaded nanoparticles, and Sorafenib drug used as a positive control, using the formula given below:

$$\%\,Cell\ viability = \frac{Absorbance\ of\ treated\ cells - absorbance\ blank}{Absorbance\ control - absorbance\ blank} \times 100$$

After that, 100 μL of DMSO was added after removing all media, and the absorbance values were recorded at both 570 and 620 nm using a microplate reader to dissolve the formazan crystals (Multiskan FC, ThermoFisher Sci., Waltham, MA, USA) [29, 32].

3 | Results and Discussion

Absorption spectrum and specificity studies were performed for aspirin and ibuprofen to determine the maximum absorption wavelength, and the specific absorption spectrum, which were found to be 225 and 264 nm, respectively. The calibration curve of the drug obeyed Beer–Lambert's law in the concentration range of 4–50 μg/mL ($R^2 = 0.99$), and results are shown in Figure 1.

The equations obtained from the calibration curve were used to calculate the actual drug concentrations to determine each drug's encapsulation efficiency.

Before initiating the synthesis of the LNPs process, the palm oil extracted with existing facilities was characterized by using GC. The fatty acid profiles of palm fruit extracts obtained from regional sources were composed of both saturated and unsaturated fatty acids, including 27.5% of lauric acid (C12:0), 12.2% of myristic acid (C14:0), 9.5% of palmitic acid (C16:0), 2.4% of stearic acid (C18:0), 37.8% of elaidic acid (C18:1 trans-9), and 10.6% of linoleic acid (C18:2). The fatty acid profiles of palm oil extracted by other techniques are similar, except for variations in the concentration of saturated and unsaturated fatty acids [33].

3.1 | Optimization Results of Drug-Loaded and Nonloaded LNPs

Aspirin- and ibuprofen-loaded LNPs were prepared by mixing each drug with two types of lipids (palm oil and thyme oil) and a surfactant (Tween80) via ultrasonication and high-speed mixing, resulting in different formulations created by Design Expert software. The various compositions of drug-loaded LNPs and their responses for encapsulation efficiency (EE%) and antibacterial activities for *E. coli* (EC, mm) and *S. aureus* (SA, mm) are summarized in Table 1. Overall, the formulations exhibited varying degrees of antibacterial activity, with EC showing inhibition zone diameters ranging from 7 to 13 mm, and SA showing diameters ranging from 7 to 14 mm. Notably, formulations containing ibuprofen generally demonstrated superior or comparable efficacy compared with those containing aspirin. The highest antibacterial activity (13 mm for EC and 14 mm for SA) was observed in Run 2, which had a drug:lipid ratio of 1:7 and an incubation time of 15 min and used ibuprofen. Conversely, the lowest inhibition zones (7 mm for both EC and SA) were recorded for Run 10, which used aspirin with a 1:2 drug-to-lipid ratio and a 10-min incubation time. The data suggest that the type of drug and the drug:lipid ratio are critical factors influencing the resulting antibacterial efficacy, with ibuprofen-loaded formulations generally providing a more potent inhibitory effect against the tested pathogens.

The encapsulation efficiency of LNPs was the primary response in all experimental studies, with the minimum and maximum values of the variables used in this design presented in Table 1. In this set of experiments, the maximum EE% of LNPs was obtained as 94%, at the point where the ibuprofen used drug:lipid ratio was 1:7 in a 5-min incubation time.

The F value of the model was determined by analysis of variance (ANOVA) to be 17.37, which indicates statistical significance ($p < 0.05$). According to the ANOVA test, significance was found

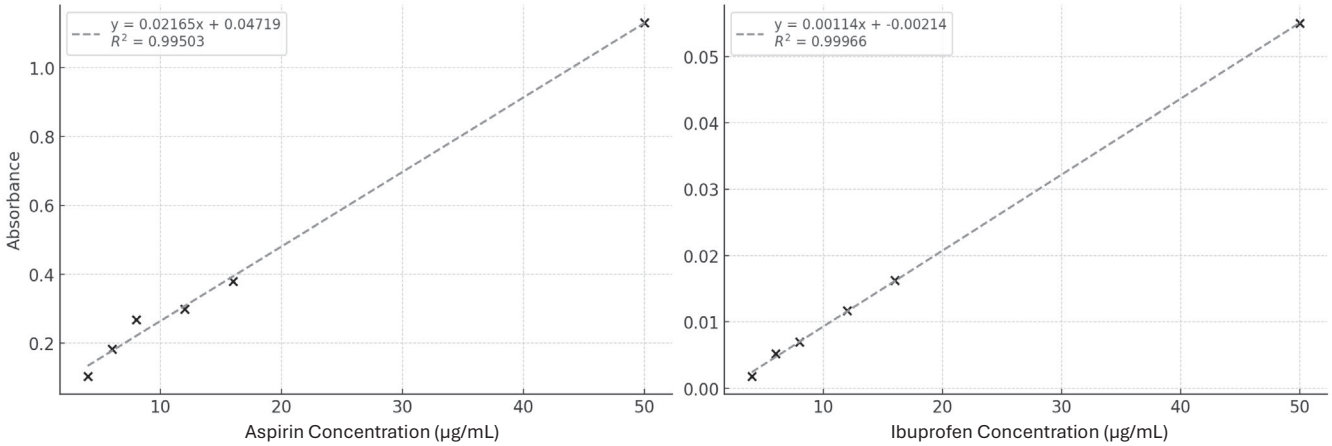

FIGURE 1 | Calibration curve for aspirin and ibuprofen.

TABLE 1 | The design of the LNPs synthesis.

	Factor 1	Factor 2	Factor 3	Response 1	Response 2	Response 3
Runs	**Drug:lipid (w:w)**	**Incubation time (min)**	**Drug**	**EE %**	**EC (mm)**	**SA (mm)**
1	1:8	10	Asp	6.0	10	9
2	1:7	15	Ibf	71.1	13	14
3	1:7	5	Ibf	94.0	13	12
4	1:5	10	Ibf	58.2	11	10
5	1:5	17	Asp	5.3	9	9
6	1:5	3	Ibf	86.0	10	10
7	1:7	5	Asp	7.4	9	9
8	1:5	10	Ibf	53.4	11	11
9	1.5	10	Asp	5.8	9	8
10	1:2	10	Asp	2.8	7	7
11	1:3	5	Asp	3.5	8	7
12	1:5	10	Asp	5.6	9	8
13	1:7	15	Asp	7.3	10	10
14	1:5	3	Asp	5.4	8	7
15	1:5	10	Ibf	40.6	12	11
16	1:3	15	Asp	3.5	8	8
17	1:5	10	Asp	5.2	8	9
18	1:2	10	Ibf	22.6	9	9
19	1:3	5	Ibf	12.2	10	11
20	1:5	17	Ibf	31.7	11	11
21	1:3	15	Ibf	20.9	10	10
22	1:8	10	Ibf	63.1	13	13

Abbreviations: Asp, aspirin; EC, *Escherichia coli*; EE, encapsulation efficiency; Ibf, Ibuprofen; SA, *Staphylococcus aureus*.

for the type of the drug, drug:lipid ratio, and the interactions of these two variables ($p < 0.05$). It is evident that the theoretical and experimental values are closely matched for the synthesis of drug-loaded LNPs, suggesting that the model was successfully developed, showing a strong correlation between the variables affecting the EE% of the nanoparticles (Table S1).

The relationship between the selected parameters and each response was established using a second-order polynomial equation (Equation 1 and 2) in terms of coded factors for the EE of aspirin and ibuprofen, respectively:

$$\text{EE\% of aspirin} = -188.92499 + 222.19551xA + 4.41942xB - 3.96084xAB - 58.29642xA^2 + 0.075744xB^2 \quad (1)$$

$$\text{EE\% of ibuprofen} = -286.99446 + 332.76337xA + 2.15166xB - 3.96087xAB - 58.29642xA^2 + 0.075744xB^2 \quad (2)$$

The statistical equation indicates that the negative values represent an antagonistic effect and the positive values have a synergistic effect on the response where "A" is drug:lipid, "B" is incubation time, and "C" is type of the drug.

The R^2 value, which is a measure of the model's fit, is close to one, thus demonstrating a strong correlation between the experimental and predicted responses [32]. With an R^2 of 0.9144, which aligns well with the adjusted R^2 of 0.8618, the model exhibits high significance.

The optimization study was conducted with the objective of maximizing the EE% following a one-way ANOVA procedure. The 3D visual of the model indicates that to increase the EE% of LNPs, a suitable ratio is 1:7 of drug to lipid, in addition to a 5-min incubation time for both drugs (Figure 2). However, it was observed that the ibuprofen-loaded LNPs exhibited a higher EE% compared with the aspirin-loaded ones. The lower EE% could be attributed to differences in saturation solubility of lipids in various solvents, the solubility of the drug in the aqueous phase, viscosity of the internal phase, and the degree of vapor pressures [34]. In studies, Pethe et al. [34] reported that aspirin-loaded PLGA nanoparticles were produced using acetone, with encapsulation effectiveness ranging from 24% to 60%, whereas Yeo et al. [35] reported a correlation between the size of the particles and the encapsulation effectiveness (EE%) in SLN. They found that the presence of H-bonds between the carbonyl group

(C=O) of curcumin and the COOH groups of lipids resulted in a disruption of the arrangement of bonds between curcumin (Cur) and lipids, leading to a reduction in EE%. In a separate study, Lemraski et al. [36] found that the adsorption of ibuprofen molecules onto Ag nanoparticles reduced surface area and pore volume, while increasing pore diameter due to the occupation of large pores, causing internal pore strain. This outcome validates this study's finding of ibuprofen's efficacy of encapsulation.

A series of experiments were conducted under optimal production conditions with the objective of validating the developed model and confirming the optimization results for LNP synthesis with both drugs. The optimal parameters included ibuprofen as the drug, a drug-to-lipid ratio of 1:7, a 5-min incubation time, and a mixing speed of 250 rpm. The harmonic mean particle diameter determined under these conditions was measured as 210 ± 10 nm.

Increasing the lipid ratio positively influenced the increase in antibacterial activity against both *E. coli* and *S. aureus* for both ibuprofen and aspirin. However, the results obtained with ibuprofen samples are superior, and only ibuprofen progressed according to expected results (Figures 3 and 4). According to Assuncao et al. [37], the amount of oil added to the nanoparticle synthesis had a significant and positive effect on particle size.

3.2 | Characterization of Drug-Loaded and Nonloaded LNPs

The surface morphology of the LNPs was examined by SEM. SEM images show that spherical-shaped particles are prevalent in both aspirin- and ibuprofen-loaded LNPs, ranging from 176.2 to 220.4 nm and 218.6 to 557.1 nm, respectively (Figure 5). These results are in accordance with the data obtained by DLS analyses.

Composite EDX analysis was performed to confirm the formation of LNPs. Separate analyses of aspirin- and ibuprofen-loaded structures were performed. Since the synthesized composite nanostructure is organic, the elements C, N, and O are prominently observed in the EDX spectrum. The values measured

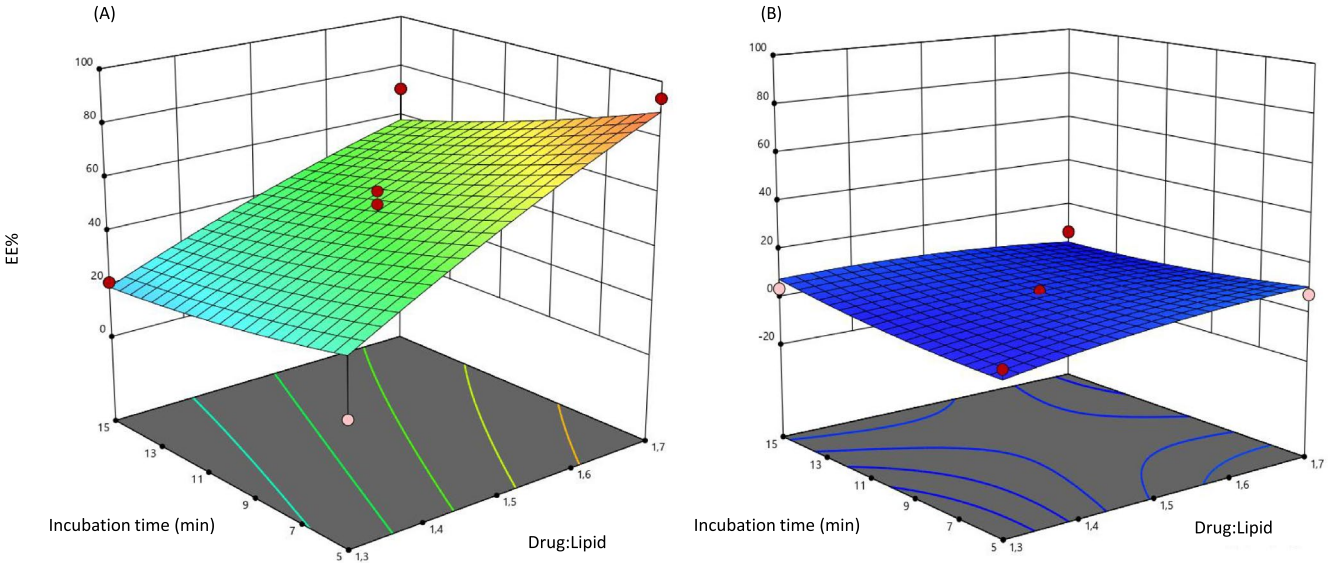

FIGURE 2 | Results for ibuprofen-loaded LNPs (A) and aspirin-loaded sample (B).

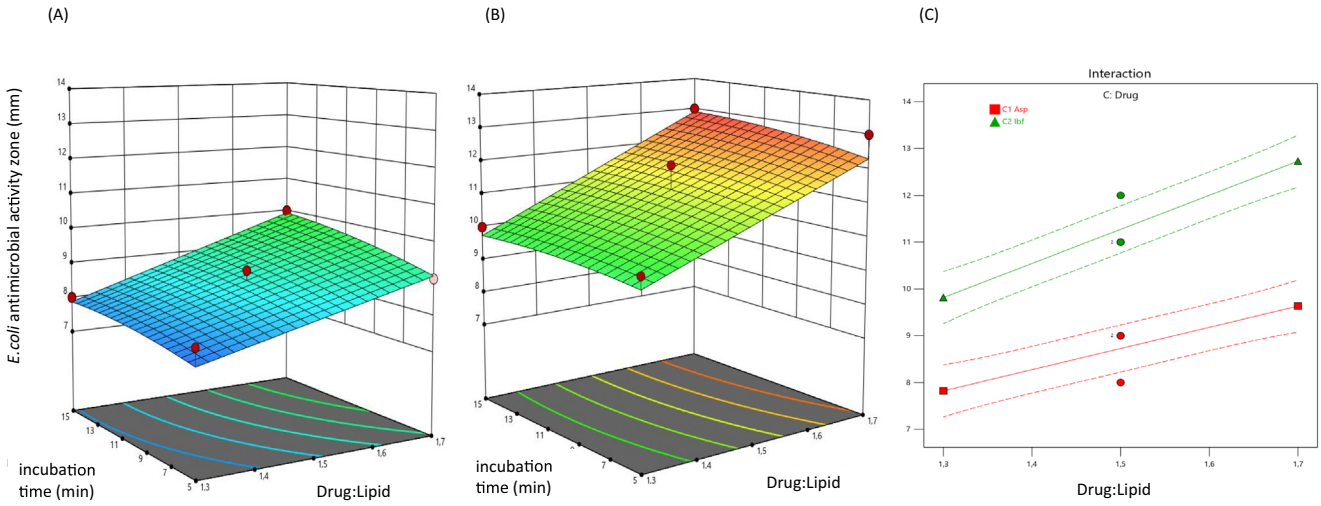

FIGURE 3 | Antibacterial zone diameter effect of (A) aspirin-loaded LNPs, (B) ibuprofen-loaded LNPs, and (C) drug interaction on *E. coli*.

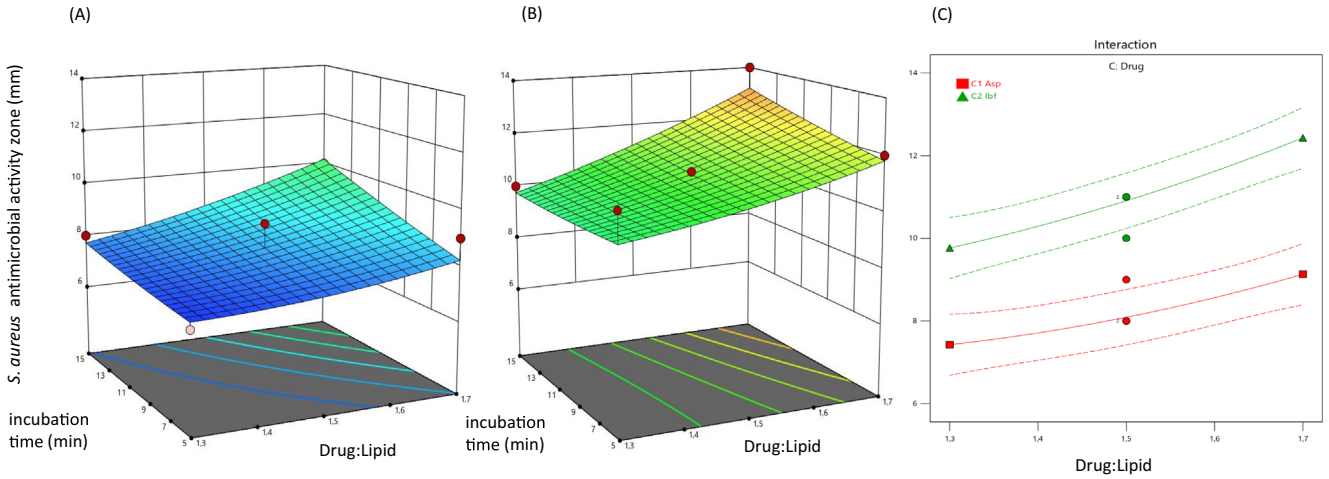

FIGURE 4 | Antibacterial zone diameter effect of (A) aspirin-loaded, (B) ibuprofen-loaded LNPs, and (C) drug interaction on *S. aureus*.

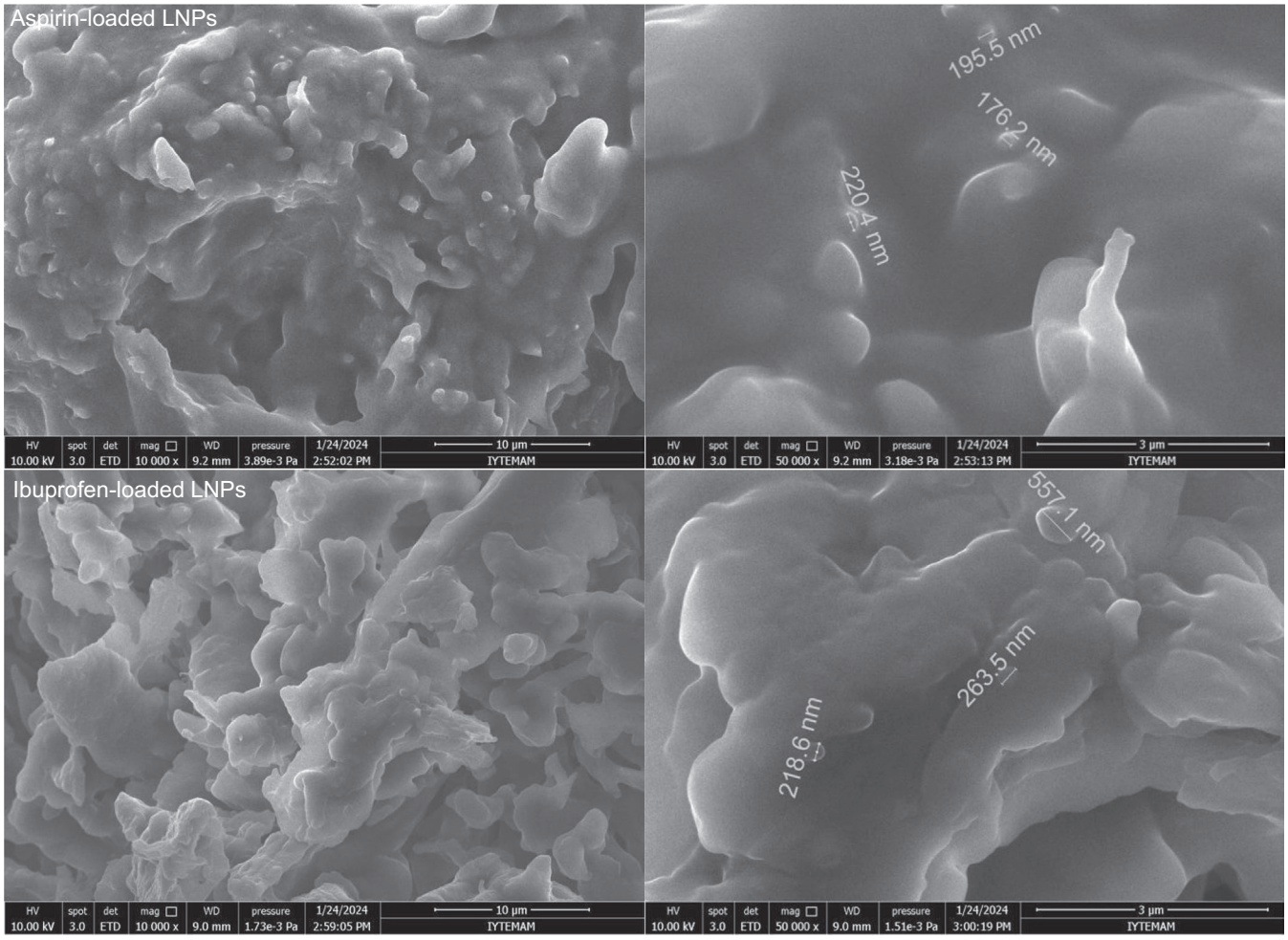

FIGURE 5 | SEM images of drug-loaded nanoparticles at 10 000× and 50 000×.

in atomic and weight percentages are detailed in the EDX spectrum and listed with eZAF Smart Quant tables shown in Figure 6. The peaks identified in the elemental analysis of aspirin- and ibuprofen-loaded nanoparticles are C (0.277 keV) and O (0.525 keV), and these peaks dominate because of the organic and oxygen-rich structure of ibuprofen ($C_{13}H_{18}O_2$), aspirin ($C_9H_8O_4$), and lipid molecules [38, 39]. Ibuprofen-loaded NP has a high carbon content because of its aromatic and alkyl groups. Oxygen peaks result from the carboxyl group (–COOH) and oxygen atoms in the molecule. Although nitrogen is not a constituent of pure ibuprofen, it may be present in formulations or excipients associated with the lipid nanoparticles [36]. In the case of aspirin-loaded NP examination, the high carbon content is due to the aromatic ring and carbon chains in aspirin. The

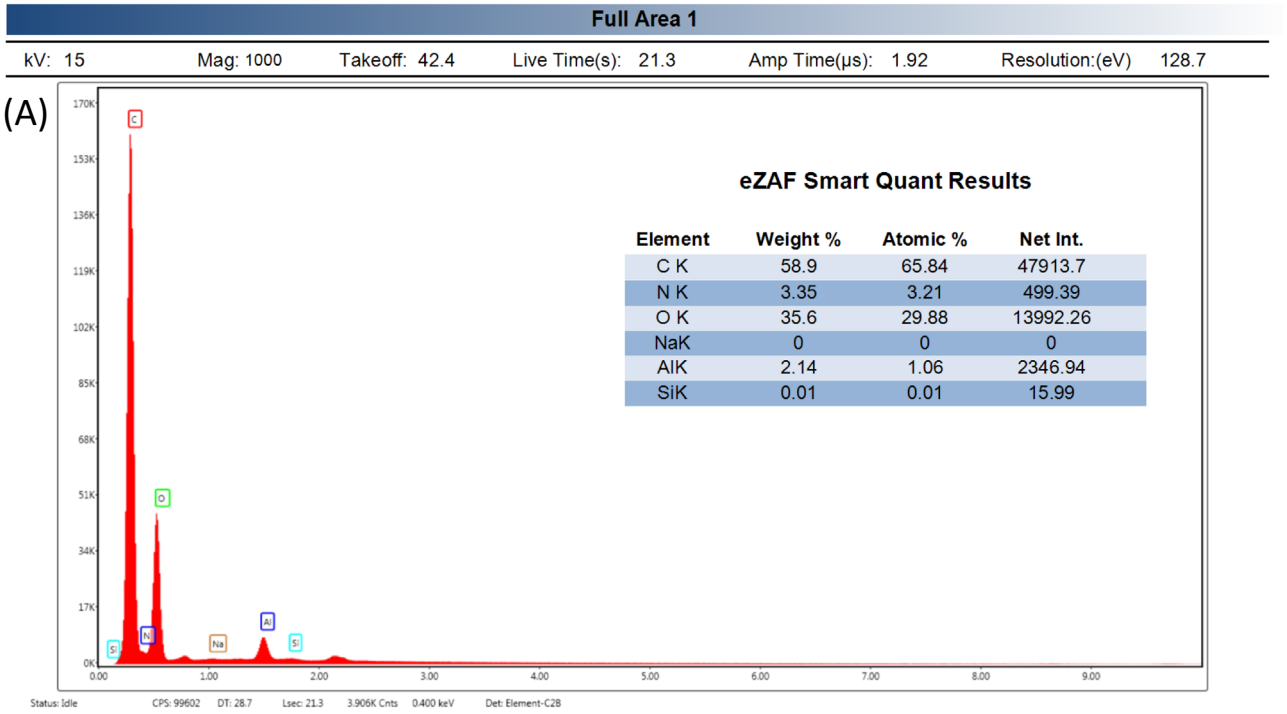

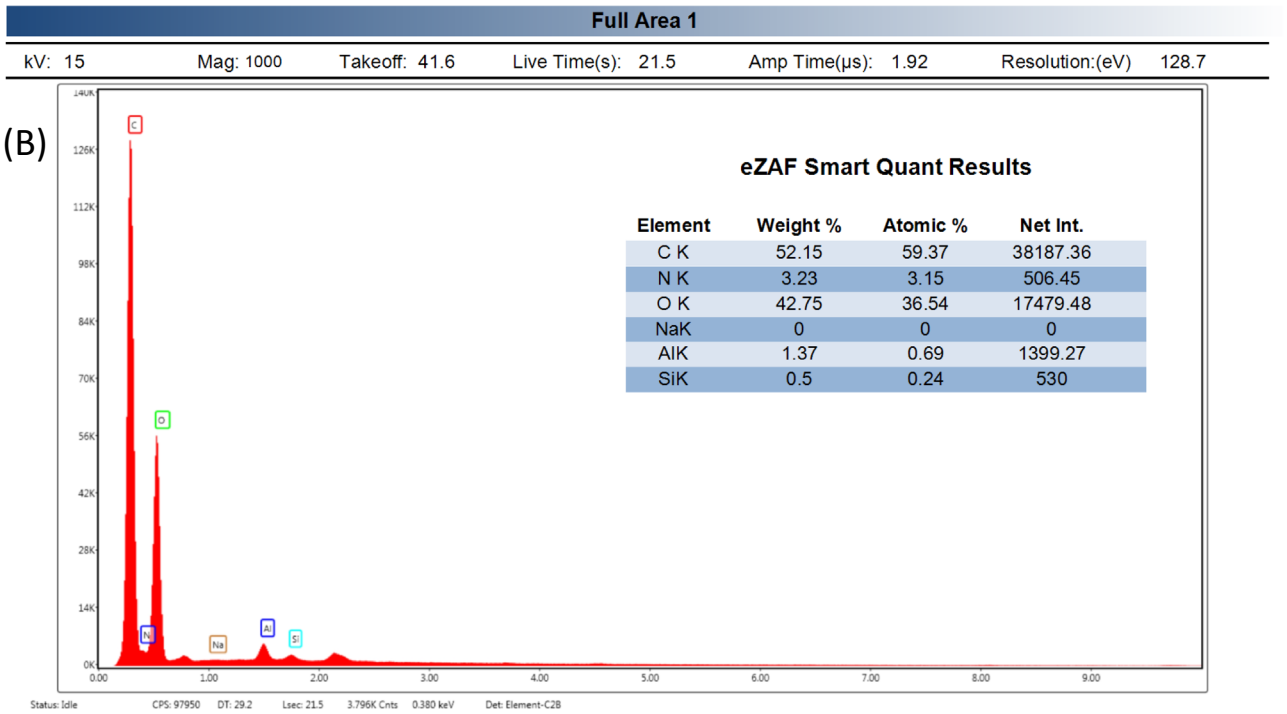

FIGURE 6 | Peaks corresponding to elements in aspirin-loaded nanoparticle (A) and peaks corresponding to elements in ibuprofen-loaded nanoparticle (B).

oxygen content corresponds to the oxygen atoms in the carboxyl group (–COOH) and the ester functional group in aspirin. In these NPs, impurities and excipients used in nanoparticle carrier systems or a substrate (e.g., silica- or sodium-based compounds) led to the observation of additional peaks for elements such as sodium (Na, ~1.04 keV) or silicon (Si, ~1.74 keV). Hydrogen (H) was not detected in EDX because of its low atomic number [39].

Particle characterization studies were conducted to evaluate the effects of various factors by using selected runs. Particle size and PDI values, which are used to determine the quality of nanoparticles, are important in influencing cell uptake of endocytosis-based drug delivery systems in various therapeutic areas such as cancer treatment [31]. PDI, also known as the homogeneity index, refers to the size distribution of particles in a sample [40].

Zeta potential, which is indicative of the electrical potential on a particle's surface, is a critical factor in determining the stability of the particles. Higher zeta potential values result in particle repulsion, thereby preventing nanoparticle aggregation and enhancing storage stability. Values exceeding ±30 mV indicate strong stability against droplet coalescence [37, 41]. Conversely, lower zeta potential values promote the release of encapsulated drugs [35, 42]. The classification of nanoparticle zeta potential ranges from −10 to +10 mV as neutral, to ≤ −30 or ≥ 30 mV as strongly anionic or cationic, respectively [41]. In this study, particle size, PDI, and zeta potential of all the formulations for aspirin ranged from 182.7 to 365.6 nm, 0.218 to 0.314, and −1.6 to −3.87 mV, respectively. Concurrently, PDI, the particle size, and zeta potential of all the formulations for ibuprofen ranged from 0.299 to 0.376, 254.8 to 526.5 nm, and −6.26 to −12.7 mV, respectively. Large positive or negative zeta potential values indicate that the sample is stable, whereas smaller values indicate low stability and potential particle aggregation because of Van der Waals interactions [37]. Aligning with the results of this study, Sabeti et al. also obtained drug-loaded palm oil–based nanoparticles with dimensions of approximately > 400 nm.

Stability was assessed by measuring nanoparticle sizes after 30 days for both aspirin- and ibuprofen-loaded LNPs, and the results of the average particle diameter were formed as 182.7 + 10.5 to 365.6 + 15.3 nm and 254.8 + 11.2 to 526.5 + 14.2 nm, respectively. Changes in particle size were minimal at the endpoint, zeta values remained positive (+30 ± 10 mV), and PDI below 0.2 indicated that all systems were homogenous [12].

According to Ribeiro et al. [41], the particle size of crude palm oil NPs with casein and gum arabic was found to be 155.66 and 177.86 nm, respectively. PDI values of palm oil NPs were below 0.2, indicating that the sample was monodispersed. Higher zeta potential values (≥ −30 mV) were observed for crude palm oil NPs. It is widely accepted that surface droplets are suitable for the maintenance of stable emulsions when they exhibit a negative electric charge in conjunction with nonionic surfactants and have values of more negative than −30 mV. Casein-based nanoparticles are smaller than drug-loaded nanoparticles, probably due to the amphiphilic structure leading to pH decrease and strong electrostatic repulsion [41]. In another study focusing on the formulation of solid lipid palm oil–based nanoparticles, an optimal formulation exhibited a particle size of 140.5 ± 1.02 nm, a PDI of 0.218 ± 0.01, and a zeta potential of 28.6 ± 8.71 mV, suggesting a stable and uniform nanoparticle system suitable for therapeutic applications [37]. Ideally, LNPs should have smaller and more uniform particle sizes, particularly for applications such as intravenous drug delivery. In addition, the effect of lipid concentration on particle size could be related to the interaction between lipids and drugs [35].

FTIR spectroscopy is a widely employed technique for the evaluation of the quality of diverse molecules and the identification of functional groups within the structural composition of a compound [43]. FTIR spectrum of nonloaded LNP and ibuprofen- and aspirin-loaded LNPs are shown in Figure 7, respectively. Generally, adsorption peaks between 3200 and 3600 cm^{-1} are due to the following: stretching and bending vibrations in bonds, N–H vibrations in peptide groups, or O–H vibrations

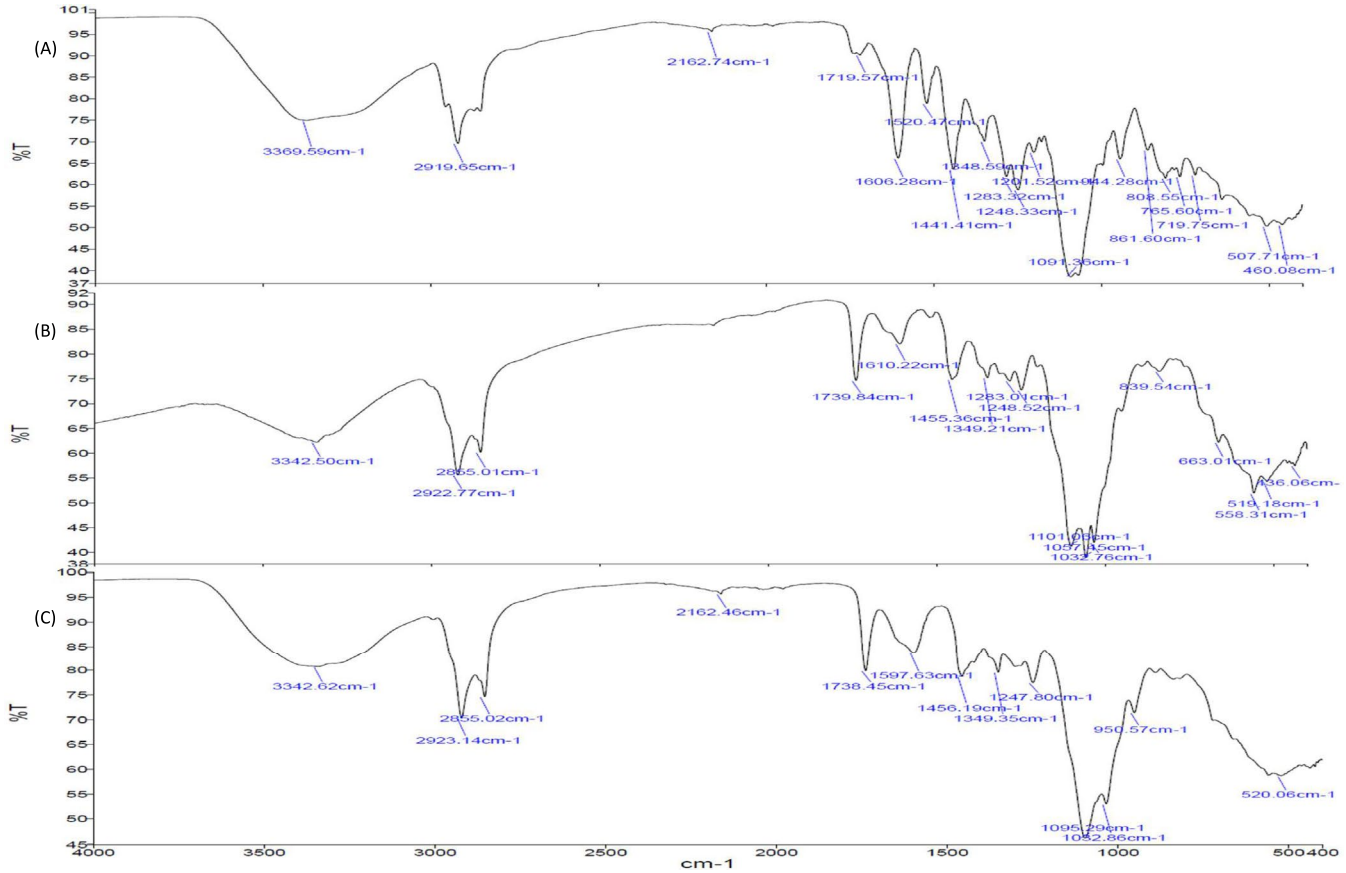

FIGURE 7 | FTIR Results of nonloaded (A), ibuprofen-loaded (B), and aspirin-loaded LNPs (C).

in alcoholic and phenolic groups. The absorption peak in the region of 2800–3000 cm^{-1} corresponds to the stretching vibrations of methyl (C–H) in aldehyde compositions that commonly occur in fats and oils. At around 1700 cm^{-1} could be due to C=O stretching. The peak at 1400–1600 cm^{-1} corresponds to stretching vibrations of C=C in aromatic rings or N–H vibrations in Type II amines. In the range of 800–1250 cm^{-1}, C–C, C–H, C–O, and C–N vibrations could occur in aliphatic amines and aromatics [44]. The spectral peaks at around 1000 cm^{-1} are due to the presence of the C–O and C–H stretching of aromatic compounds [37, 44–48]. Using FTIR spectra, it was possible to directly detect crucial functional groups such as ketones (C=O stretching at 1750–1625 cm^{-1}), carboxylic acid (C=O stretching at 1730–1650 cm^{-1} and O–H stretching bonded by hydrogen at 3400–2400 cm^{-1}), and aldehydes (C=O stretching at 1750–1625 cm^{-1}, C=O stretching in C–H at 2850–2800 cm^{-1}, and C=O stretching in C–H at 2750–2700 cm^{-1}) [37].

In this study, the FTIR spectrum of nonloaded LNPs showed characteristic peaks at 3370 (O–H stretching), 2920 (C–H stretching), 2163 (C=C stretching), 1720 (C=O stretching), 1606 (C=O stretching), and 1521 cm^{-1} (C=C in aromatic rings, COOH stretching), as summarized in Figure 7. Ibuprofen-loaded LNPs have bands at 3345 cm^{-1} (O–H stretching), 2854–2923 cm^{-1} (C–H stretching), and also around 2800 cm^{-1}. These could be due to the stretching of C=O bonds in ketones, 1740 cm^{-1} (C=O stretching), around 1456–1610 cm^{-1} (C=C in aromatic rings, COOH stretching), around 1200 cm^{-1} (C–C, C–H, C–O, or C–N stretching), and around 1000 cm^{-1} (stretching of C–H bonds in aromatic rings). Pham et al. [49] reported that ibuprofen-loaded SLNs have absorption peaks at wavelengths of 1720 cm^{-1} (COOH stretching) and 1230 cm^{-1} (C=C group of aromatic rings). The intensity of the characteristic peak of ibuprofen at 1720 cm^{-1} can vary according to the interaction between the –COOH group in ibuprofen molecules and –OH group in other molecules. This result also explains the decreases in LNPs' particle size and the increase of encapsulation efficiency [49]. Aspirin-loaded LNPs spectral peaks determined at 3342.62 cm^{-1} (O–H stretching), 2855–2923 cm^{-1} (C–H stretching), 2163 (C=C stretching), 1739 cm^{-1} (C=O stretching), around 1598 cm^{-1} (C=O stretching), around 1400 cm^{-1} (C=C in aromatic rings, COOH stretching), and around 1000 cm^{-1} (stretching of C–H bonds in aromatic rings). Elmowafy et al. [50] explored the potential of quercetin/aspirin-loaded chitosan nanoparticles, similar to the current study [50]. According to Yeo et al. [35], the FTIR spectra of palmitic acid, stearic acid, and lauric acid showed characteristic peaks at 2850 and 2918 (CH_2–CH_3 stretching), 1702 (C=O), and 1465 cm^{-1} (COOH stretching). The spectra were similar among the analyzed samples, and both drug-loaded and nonloaded LNPs showed characteristic peaks of the constituents present in the formulations. Also, the OH ions in the environment play a role in both stabilization of LNPs. These conditions prevent aggregation and produce a greater number of nucleation sites [51]. According to Shahab-Navae [44], the presence of these peaks across all three samples indicates the presence of a wide range of metabolites, especially phenolic and flavonoid compounds [44].

3.3 | In Vitro Cytotoxicity Assay

The in vitro cytotoxicity assay of palm oil–based nanoparticles is a crucial step in evaluating their biocompatibility and potential for biotechnological applications. In this process, the MTT method was used to assess in vitro cytotoxicity activity of ibuprofen- and aspirin-loaded LNPs against the hepatocarcinoma cell line (Huh7). The control group exhibits the highest cell viability at 100%, as expected. Treatments with ibuprofen significantly reduce cell viability, with Ibu (100 μM) and Ibu (50 μM) showing approximately 50% and 60% viability, respectively. Similarly, aspirin treatment decreases cell viability, with Asp (100 μM) and Asp (50 μM) yielding roughly 65% and 70% viability. Sorafenib demonstrates the most potent cytotoxic effect, reducing cell viability to approximately 30%. These results suggest a dose-dependent cytotoxic effect for ibuprofen and aspirin and a notably stronger effect of sorafenib (Figure 8).

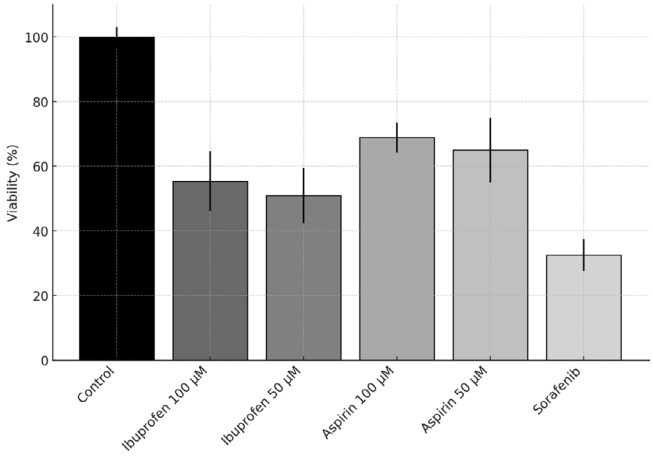

FIGURE 8 | %cell viability under different treatment conditions, including a control group, two concentrations (100 and 50 μM) of ibuprofen and aspirin, and sorafenib drug.

The size, surface charge, and composition of nanoparticles have been shown to significantly influence their interaction with cells. Owing to their lipid composition, palm oil–based nanoparticles are generally expected to exhibit low toxicity and high biocompatibility, making them potentially effective in drug delivery systems. However, it is important to carefully assess factors such as particle aggregation, oxidative stress induction, and cellular uptake efficiency. Additionally, dose-dependent toxicity patterns should be analyzed to identify any potential cytotoxic thresholds. The findings from this study contribute to the broader understanding of the suitability of palm oil–based nanoparticles in pharmaceutical and nutraceutical applications [6, 12, 42, 50, 52, 53].

4 | Conclusion

This study successfully optimized, for the first time as a region-specific output, the synthesis and characterization of LNPs loaded with aspirin and ibuprofen using locally sourced palm oil and thyme oil. The utilization of regional palm oil as a lipid component contributes to the sustainability and biocompatibility of the formulation, while enhancing drug encapsulation efficiency and antibacterial activity. The research findings demonstrate that the maximum EE% of 94% and two times higher antibacterial effectiveness compared with aspirin-loaded LNPs were achieved using ibuprofen at a drug:lipid ratio of 1:7 with a 5-min incubation time. The successful inclusion of both aspirin and ibuprofen resulted in a strong negative

surface charge (up to −15 mV) and produced formulations with average particle sizes ranging from 180 to 560 nm. In conclusion, the physicochemical characterization of the drug-loaded LNPs demonstrated key attributes suitable for targeted delivery. Specifically, ibuprofen- and aspirin-loaded LNPs exhibited promising cytotoxic effects on the hepatocarcinoma cell line (Huh7), showing 50% and 70% viability at a concentration of 50 μM, respectively. Ultimately, the optimized palmitic acid–incorporated LNP formulations, exhibiting high EE% and superior stability, demonstrate considerable promise for enhancing the clinical therapeutic efficacy of antitumor drugs. This study introduces an innovative and sustainable approach to synthesizing nanoparticles using palm oil derivatives, which significantly enriches the existing literature and highlights potential applications in areas such as targeted drug delivery for cancer and the management of infectious diseases. Moving forward, future research should prioritize in vivo evaluations and rigorously assess the long-term stability and bioavailability of these nanoparticles. It should also explore the scalability of the formulation to facilitate clinical translation and expansion into other therapeutic areas, such as tissue repair.

Author Contributions

All authors contributed to the study conception and design. **Gulizar Caliskan:** conceptualization, formal analysis, methodology, supervision, resources, investigation, writing – original draft, writing – review and editing. **Smyrna Ergonul:** data curation, formal analysis, methodology, resources, writing – original draft. **Zuhal Naz Cansu:** data curation, formal analysis, methodology, resources, writing – original draft. **Busra Kaplan:** data curation, formal analysis, methodology, resources, writing – original draft.

Acknowledgments

The authors would like to express their gratitude to Izmir University of Economics for the provision of laboratory facilities and to TÜBİTAK 2209-A—Research Project Support Programme for Undergraduate Students (grant number 1919B012222075) for financial support of this study. The present article has been prepared within the context of the bachelor's degree programme of Smyrna Ergonul, Zuhal Naz Cansu, and Busra Kaplan.

Funding

This work was supported by the TÜBİTAK 2209-A—Research Project Support Programme for Undergraduate Students (grant number 1919B012222075).

Ethics Statement

This is an observational study. There is no ethical approval required.

Consent

The authors have nothing to report.

Conflicts of Interest

The authors declare no conflicts of interest.

Data Availability Statement

The data that support the findings of this study are available on request from the corresponding author. The data are not publicly available due to privacy or ethical restrictions.

References

1. L. A. Bors and F. Erdő, "Overcoming the Blood–Brain Barrier. Challenges and Tricks for CNS Drug Delivery," *Scientia Pharmaceutica* 87, no. 1 (2019): 6.

2. M. M. Hegde, S. Prabhu, S. Mutalik, A. Chatterjee, J. S. Goda, and B. S. Satish Rao, *Multifunctional Lipidic Nanocarriers for Effective Therapy of Glioblastoma: Recent Advances in Stimuli-Responsive, Receptor and Subcellular Targeted Approaches*, vol. 52, (Springer, 2022).

3. Y. Panahi, M. Farshbaf, M. Mohammadhosseini, et al., *Recent Advances on Liposomal Nanoparticles: Synthesis, Characterization and Biomedical Applications*, vol. 45, (Taylor and Francis Ltd, 2017).

4. F. Pourgholi, J. N. Farhad, H. S. Kafil, and M. Yousefi, "Nanoparticles: Novel Vehicles in Treatment of Glioblastoma," *Biomedicine & Pharmacotherapy* 77 (2016): 98–107.

5. C. A. Wood, S. Han, C. S. Kim, et al., "Clinically Translatable Quantitative Molecular Photoacoustic Imaging With Liposome-Encapsulated ICG J-Aggregates," *Nature Communications* 12 (2021): 5410.

6. L. Xu, X. Wang, G. Yang, et al., "Development of a Concentration-Controlled Sequential Nanoprecipitation for Making Lipid Nanoparticles With High Drug Loading," *Aggregate* 4 (2023): 1–14.

7. P. Couvreur, S. Lepetre-Mouelhi, E. Garbayo, and M. J. Blanco-Prieto, "Self-Assembled Lipid-Prodrug Nanoparticles for the Treatment of Severe Diseases."

8. P. Ganesan and D. Narayanasamy, "Lipid Nanoparticles: Different Preparation Techniques, Characterization, Hurdles, and Strategies for the Production of Solid Lipid Nanoparticles and Nanostructured Lipid Carriers for Oral Drug Delivery," *Sustainable Chemistry and Pharmacy* 6 (2017): 37–56.

9. R. Tenchov, R. Bird, A. E. Curtze, and Q. Zhou, *Lipid Nanoparticles From Liposomes to MRNA Vaccine Delivery, a Landscape of Research Diversity and Advancement*, vol. 15, (American Chemical Society, 2021).

10. P. Upadhyay, R. Aslam, V. Tiwari, and S. Upadhyay, "Lipid-Based Nanocarrier Drug Delivery Approach for Biomedical Application," *Current Nanomaterials* 9 (2024): 92–108.

11. D. Istrati, I. Lacatusu, N. Bordei, et al., "Phyto-Mediated Nanostructured Carriers Based on Dual Vegetable Actives Involved in the Prevention of Cellular Damage," *Materials Science and Engineering C* 64 (2016): 249–259.

12. I. Lacatusu, N. Badea, G. Badea, et al., "Lipid Nanocarriers Based on Natural Oils With High Activity Against Oxygen Free Radicals and Tumor Cell Proliferation," *Materials Science and Engineering C* 56 (2015): 88–94.

13. V. A. Duong, T. T. Nguyen, and H. J. Maeng, "Preparation of Solid Lipid Nanoparticles and Nanostructured Lipid Carriers for Drug Delivery and the Effects of Preparation Parameters of Solvent Injection Method," *Molecules* 25, no. 20 (2020): 4781.

14. S. Nagalakshmi, S. Shanmuganathan, B. Anbarasan, and K. Sandhya, "Nanostructured Lipid Carriers (NLCs): A Novel Based Nano Carrier for Drug Delivery and Drug Targeting," *Advanced Journal of Pharmacy and Life Science Research* 4 (2016): 17–24.

15. L. N. D. M. Ribeiro, V. M. Couto, L. F. Fraceto, and E. De Paula, "Use of Nanoparticle Concentration as a Tool to Understand the Structural Properties of Colloids," *Scientific Reports* 8 (2018): 982.

16. A. C. Ortiz, O. Yañez, E. Salas-Huenuleo, and J. O. Morales, "Development of a Nanostructured Lipid Carrier (NLC) by a Low-Energy Method, Comparison of Release Kinetics and Molecular Dynamics Simulation," *Pharmaceutics* 13 (2021): 531.

17. D. Efendy Goon, S. H. Sheikh Abdul Kadir, N. A. Latip, S. A. Rahim, and M. Mazlan, "Palm Oil in Lipid-Based Formulations and Drug Delivery Systems," *Biomolecules* 9(2):64 (2019): 64.

18. R. Jeitler, C. Glader, C. Tetyczka, et al., "Investigation of Cellular Interactions of Lipid-Structured Nanoparticles With Oral Mucosal Epithelial Cells," *Frontiers in Molecular Biosciences* 9 (2022): 1–14.

19. H. J. Lim, W. K. Cheng, K. W. Tan, and L. J. Yu, "Oil Palm-Based Nanocellulose for a Sustainable Future: Where Are We Now?," *Journal of Environmental Chemical Engineering* 10, no. 2 (2022): 107271.

20. Y. He, R. F. de Araújo Júnior, R. S. Cavalcante, et al., "Effective Breast Cancer Therapy Based on Palmitic Acid-Loaded PLGA Nanoparticles," *Biomaterials Advances* 145 (2023): 213270.

21. Y. Xie, Z. Jin, D. Ma, T. H. Yin, and K. Zhao, "Palmitic Acid- and Cysteine-Functionalized Nanoparticles Overcome Mucus and Epithelial Barrier for Oral Delivery of Drug," *Bioengineering & Translational Medicine* 8 (2023): e10510.

22. V. K. Kamboj and P. K. Verma, "Palmitic Acid–Pluronic F127–Palmitic Acid Pentablock Copolymer as a Novel Nanocarrier for Oral Delivery of Glipizide," *Turkish Journal of Pharmaceutical Sciences* 16 (2019): 265–272.

23. L. E. Ordóñez-Santos, L. X. Pinzón-Zarate, and L. O. González-Salcedo, "Optimization of Ultrasonic-Assisted Extraction of Total Carotenoids From Peach Palm Fruit (*Bactris gasipaes*) By-Products With Sunflower Oil Using Response Surface Methodology," *Ultrasonics Sonochemistry* 27 (2015): 560–566.

24. D. Abril, Y. Mirabal-Gallardo, A. González, et al., "Comparison of the Oxidative Stability and Antioxidant Activity of Extra-Virgin Olive Oil and Oils Extracted From Seeds of Colliguaya Integerrima and *Cynara cardunculus* Under Normal Conditions and After Thermal Treatment," *Antioxidants* 8 (2019): 470.

25. Ü. Erdoğan and E. H. Gökçe, "Fig Seed Oil-Loaded Nanostructured Lipid Carriers: Evaluation of the Protective Effects Against Oxidation," *Journal of Food Processing and Preservation* 45 (2021): e15835.

26. K. Manjunath and V. Venkateswarlu, "Pharmacokinetics, Tissue Distribution and Bioavailability of Clozapine Solid Lipid Nanoparticles After Intravenous and Intraduodenal Administration," *Journal of Controlled Release* 107 (2005): 215–228.

27. S. M. Martins, T. Wendling, V. M. F. Gonçalves, B. Sarmento, and D. C. Ferreira, "Development and Validation of a Simple Reversed-Phase HPLC Method for the Determination of Camptothecin in Animal Organs Following Administration in Solid Lipid Nanoparticles," *Journal of Chromatography B: Analytical Technologies in the Biomedical and Life Sciences* 880 (2012): 100–107.

28. S. M. Martins, B. Sarmento, C. Nunes, M. Lúcio, S. Reis, and D. C. Ferreira, "Brain Targeting Effect of Camptothecin-Loaded Solid Lipid Nanoparticles in Rat After Intravenous Administration," *European Journal of Pharmaceutics and Biopharmaceutics* 85 (2013): 488–502.

29. G. Caliskan, T. Mutaf, H. C. Agba, and M. Elibol, "Green Synthesis and Characterization of Titanium Nanoparticles Using Microalga, *Phaeodactylum tricornutum*," *Geomicrobiology Journal* 39 (2022): 83–96.

30. E. Ilhan-Ayisigi, F. Ulucan, E. Saygili, P. Saglam-Metiner, S. Gulce-Iz, and O. Yesil-Celiktas, "Nano-Vesicular Formulation of Propolis and Cytotoxic Effects in a 3D Spheroid Model of Lung Cancer," *Journal of the Science of Food and Agriculture* 100 (2020): 3525–3535.

31. X. Zhang, X. Hou, L. Ma, Y. Shi, D. Zhang, and K. Qu, "Analytical Methods for Assessing Antimicrobial Activity of Nanomaterials in Complex Media: Advances, Challenges, and Perspectives," *Journal of Nanobiotechnology* 21, no. 1 (2023): 97.

32. A. Atik, T. Günal, P. A. Bozkurt, et al., "Characterization of Cisplatin Loaded Hydrophilic Glycol Chitosan Modified Eumelanin Nanoparticles for Potential Controlled-Release Application," *Journal of Drug Delivery Science and Technology* 84 (2023): 104440.

33. A. Kumar, A. Ahuja, J. Ali, and S. Baboota, "Curcumin-Loaded Lipid Nanocarrier for Improving Bioavailability, Stability and Cytotoxicity Against Malignant Glioma Cells," *Drug Delivery* 23 (2016): 214–229.

34. A. Pethe, A. Shanbhag, A. Sherje, and S. Agrawal, "Formulation and Evaluation of Aspirin-Loaded PLGA Nanoparticles for Ophthalmic Use," *International Journal of Applied Pharmaceutics* 15 (2023): 161–165.

35. S. Yeo, M. J. Kim, Y. K. Shim, I. Yoon, and W. K. Lee, "Solid Lipid Nanoparticles of Curcumin Designed for Enhanced Bioavailability and Anticancer Efficiency," *ACS Omega* 7 (2022): 35875–35884.

36. E. G. Lemraski, S. Alibeigi, and Z. Abbasi, "Ibuprofen@silver Loaded on Poly (Vinyl Alcohol)/Chitosan Co-Polymer Scaffold as a Novel Drug Delivery System," *Materials Today Communications* 33 (2022): 104311.

37. L. S. Assunçao, C. Oliveria de Souza, F. Shahidi, et al., "Optimization and Characterization of Interspecific Hybrid Crude Palm Oil Unaué HIE OxG Nanoparticles With Vegetable By-Products as Encapsulants," *Food* 13 (2024): 5–23.

38. National Center for Biotechnology Information, "PubChem Compound Summary for CID 3672, Ibuprofen," (2025).

39. J. I. Goldstein, D. E. Newbury, P. Echlin, et al., *Scanning Electron Microscopy and X-Ray Microanalysis*, 3rd ed., (Springer, 2003).

40. M. Danaei, M. Dehghankhold, S. Ataei, et al., "Impact of Particle Size and Polydispersity Index on the Clinical Applications of Lipidic Nanocarrier Systems," (2018): 1–17.

41. C. D. Ribeiro, F. B. Schappo, I. da Silva Sales, et al., "Novel Bioactive Nanoparticles From Crude Palm Oil and Its Fractions as Foodstuff Ingredients," *Food Chemistry* 373 (2022): 131252.

42. A. M. Araya-Sibaja, N. J. Salazar-López, K. W. Romero, et al., "Use of Nanosystems to Improve the Anticancer Effects of Curcumin," *Beilstein Journal of Nanotechnology* 12, no. 1 (2021): 1047–1062.

43. S. Suresh, S. Karthikeyan, and K. Jayamoorthy, "FTIR and Multivariate Analysis to Study the Effect of Bulk and Nano Copper Oxide on Peanut Plant Leaves," *Journal of Science: Advanced Materials and Devices* 1 (2016): 343–350.

44. F. Shahab-Navaei and A. Asoodeh, "Synthesis of Optimized Propolis Solid Lipid Nanoparticles With Desirable Antimicrobial, Antioxidant, and Anti-Cancer Properties," *Scientific Reports* 13 (2023): 18290.

45. L. A. Frank, "Chitosan as a Coating Material for Nanoparticles Intended for Biomedical Applications," *Reactive and Functional Polymers* 147 (2020): 104459.

46. H. E. Salama and M. S. Abdel Aziz, "Optimized Carboxymethyl Cellulose and Guanidinylated Chitosan Enriched With Titanium Oxide Nanoparticles of Improved UV-Barrier Properties for the Active Packaging of Green Bell Pepper," *International Journal of Biological Macromolecules* 165 (2020): 1187–1197.

47. R. Dobrucka, "Synthesis of Titanium Dioxide Nanoparticles Using *Echinacea purpurea* Herba," *Iranian Journal of Pharmaceutical Research* 16 (2017): 753–759.

48. B. K. Thakur, A. Kumar, and D. Kumar, "Green Synthesis of Titanium Dioxide Nanoparticles Using *Azadirachta indica* Leaf Extract and Evaluation of Their Antibacterial Activity," *South African Journal of Botany* 124 (2019): 223–227.

49. C. V. Pham, M. C. Van, H. P. Thi, et al., "Development of Ibuprofen-Loaded Solid Lipid Nanoparticle-Based Hydrogels for Enhanced In Vitro Dermal Permeation and In Vivo Topical Anti-Inflammatory Activity," *Journal of Drug Delivery Science and Technology* 57 (2020): 101758.

50. M. Elmowafy, K. Shalaby, M. H. Elkomy, et al., "Exploring the Potential of Quercetin/Aspirin-Loaded Chitosan Nanoparticles Coated With Eudragit L100 in the Treatment of Induced-Colorectal Cancer in Rats," *Drug Delivery and Translational Research* 13 (2023): 2568–2588.

51. G. K. Rose, R. Soni, P. Rishi, and S. K. Soni, "Optimization of the Biological Synthesis of Silver Nanoparticles Using Penicillium Oxalicum GRS-1 and Their Antimicrobial Effects Against Common Food-Borne Pathogens," *Green Processing and Synthesis* 8 (2019): 144–156.

52. D. Cao, X. Shu, D. Zhu, S. Liang, M. Hasan, and S. Gong, "Lipid-Coated ZnO Nanoparticles Synthesis, Characterization and Cytotoxicity Studies in Cancer Cell," *Nano Convergence* 7 (2020): 14.

53. L. V. Arsenie, I. Lacatusu, O. Oprea, N. Bordei, M. Bacalum, and N. Badea, "Azelaic Acid-Willow Bark Extract-Panthenol–Loaded Lipid Nanocarriers Improve the Hydration Effect and Antioxidant Action of Cosmetic Formulations," *Industrial Crops and Products* 154 (2020):112658.

Supporting Information

Additional supporting information can be found online in the Supporting Information section. **Table S1:** Results of the ANOVA for encapsulation efficiency.